

Cellular level MR Phase Contrast Microscopy and MEMRI of MnCl₂ labeled tumor cells with direct optical correlation

N. Baxan¹, U. Kahlert², J. Hennig¹, and D. von Elverfeldt¹

¹Dept. of Radiology, Medical Physics, University Medical Center Freiburg, Freiburg, Germany, ²Department of Stereotactic Neurosurgery, University Medical Center Freiburg, Freiburg, Germany

INTRODUCTION: Susceptibility differences between tissues were recently used for bringing up a new type of contrast in MRI, different from the conventional T_1 , T_2 or spin density, known as phase contrast [1]. This method showed improved image contrast of human or rodent neuroarchitecture *in vivo* [2], however, with unavailable direct phase imaging of cellular architecture. In this study, we present for the first time the ability of the microcoil-based phase contrast MRI to resolve cellular structure of human glioma neurospheres, at significantly improved resolutions ($10 \times 10 \mu\text{m}^2$) with direct optical image correlation. Furthermore, after cell labeling with manganese chloride ($MnCl_2$) [3], the paramagnetic properties of this intracellular contrast agent were exploited using phase imaging to further enhance the contrast of cell structure. The $MnCl_2$ property to function as a T_1 contrast agent, enabled to look closer into cell physiology with MRI: temporal changes of $MnCl_2$ uptake, retention and release time within and from single cells and individual clusters were assessed.

MATERIALS AND METHODS: Brain tumor samples of patients with glioma were collected following surgical resection under institutional review board-approved protocols. The cell lines were from a Glioblastoma multiform (WHO IV). Immediately after dispensing the cells (10^5 cells/ μl in $\sim 2 \mu\text{l}$ medium) on the surface of a planar microcoil (500 μm inner diameter, *Bruker Switzerland*), the sample container was closed with an adhesive film against evaporation. Experiments were performed on a 9.4T Bruker Biospec animal scanner; 2D multi-slice GE images were acquired with: TR/TE = 400/12 ms, in plane resolution $10 \times 10 \mu\text{m}^2$, slice thickness 170 μm ; BW: 27.7 kHz; acq. time: 13 min 39 s. Images were processed offline with custom-made software developed in Matlab to reconstruct the magnitude and phase images. The background field inhomogeneity resulting from imperfect shimming was removed by applying a high pass filter for the phase image preserving the small-scale phase variations caused by local cellular structure [4]. T_1 -weighted micro-images were acquired using a 3D MP-RAGE sequence: inversion time IT: 4367 ms; TR/TE: 8728/8.8 ms, segment number: 1; resolution: $12 \times 16 \times 80 \mu\text{m}^3$; acq. time: 4 min 39 s. The $MnCl_2$ uptake, retention and wash-out time was investigated in individual clusters and single cells exposed to increasing $MnCl_2$ concentrations ranging from 0.1 to 1 mM (5 concentrations, 1h incubation) and was quantitatively assessed by measuring the contrast to noise ratio (CNR) at different time points (1, 2, 3, 6, 18 and 40 h post $MnCl_2$ exposure). Representative T_1 images of labelled clusters at several time points are displayed in fig. 2. The samples were afterwards examined and imaged via light microscopy (AxioImager A1, Zeiss, Germany) thus providing a template to correlate the acquired MR images with.

RESULTS/DISCUSSION

The benefits of using the phase signal information for revealing the structure of cellular clusters is illustrated in fig 1. The correct rendering of cellular structure on the phase contrast images was confirmed by the optical micrograph taken from the same sample. The contrast of high-pass filtered phase images (*B*, 2nd column) enabled a better definition of cluster boundaries compared to the magnitude and T_1 weighted images of non-labeled cells (Fig.1B-*i*). The MR phase contrast accuracy to exhibit cellular structure at this level of resolution was quantitatively assessed by measuring the cluster size on the high-pass filtered phase and corresponding optical microscopy images. The phase images of both labeled (Fig. 1B-*ii*, *iii*) and non-labeled clusters reveal accurate information on cluster size and location with no significant difference between cluster diameter measured from both phase and microscope images ($p=0.94$, $n=9$) (Fig. 1A). Conversely, the magnitude image does not provide reliable cluster discrimination. The definition of edges is considerably reduced in the magnitude case with cluster size significantly lower ($p=0.0002$, $n=4$) than in the light microscope images (images not shown). Details in the magnitude image are lost as several clusters are not detectable (fig 1B-*i*th column). The $MnCl_2$ uptake in individual cells and clusters was found dose dependent with a close relation among CNR changes, $MnCl_2$ concentrations and cell/cluster size. MRI showed a fast uptake of $MnCl_2$ immediately after labelling (signal loss) followed by a slow contrast agent release during several hours. Cell exposure to 0.1 mM resulted in maximal CNR (=36) on the T_1 -weighted images at 2 h post $MnCl_2$ incubation. There was an indication of signal saturation at higher doses (> 0.2 mM) at 2 h post $MnCl_2$ exposure (see Fig 2, 2nd row). The signal loss in single cells and individual clusters could be linked with a rapid decay of T_2 relaxation time at high $MnCl_2$ dose exposure. This could explain the remaining dark spots in the inner part of clusters labelled with 0.3 mM $MnCl_2$ and imaged at 18 h post exposure (arrow, fig 1B-*ii*).

At this time point the highest CNR was found 3 times lower than at 0.1mM followed by a slow contrast agent release (increased T_1 contrast of the medium). Preliminary experiments show that even at 40 h post labelling (fig. 2, bottom row) the contrast is still superior compared to the baseline (non-labelled cells). Viability tests based on Trypan blue exclusion assay confirmed $MnCl_2$ biological compatibility at 1 to 48h after labelling.

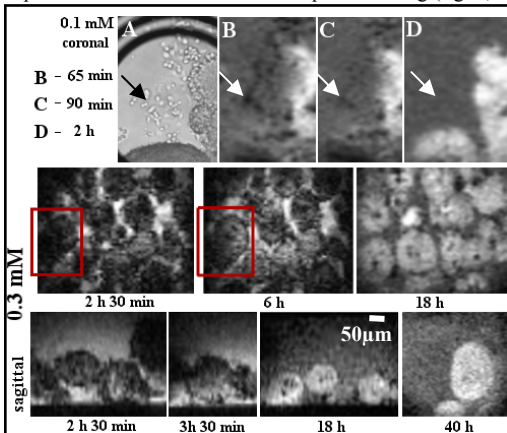


Figure 2: T_1 -weighted images of clusters labeled with 0.1 and 0.3 mM $MnCl_2$ showing contrast changes measured at different time points. White arrows point out fast uptake in single cells at 1 h after labeling (B, signal loss) followed by $MnCl_2$ release (D).

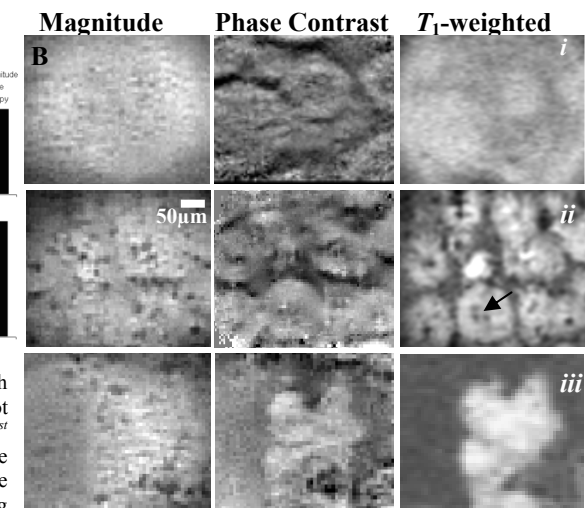


Figure 1: (A) Measured cluster size from magnitude, phase and optical images prove the accuracy of MR phase contrast microscopy. (B) Magnitude, Phase Contrast and T_1 -weighted images of glioblastoma cell clusters. (i) non-labeled cells, (ii)-0.3 mM at 18 h after $MnCl_2$ exposure; (iii)-0.1 mM at 2 h after $MnCl_2$ exposure.

CONCLUSIONS: Based on these findings, the methods presented herein offer a practical way of comparing the effectiveness and accuracy of the phase contrast technique in performing morphological imaging at cellular-level resolutions. These preliminary results suggest phase imaging as a potential candidate to explore MEMRI since the contrast was found to be enhanced by both $MnCl_2$ uptake and increased SNR due to a reduction in T_1 . Furthermore, knowing the optimal $MnCl_2$ concentration for improved signal enhancement in MRI may help when setting up new strategies for performing *in vivo* MR molecular and cellular imaging. In conclusion, the association between highly sensitive microcoils, phase contrast μ MRI and $MnCl_2$ labeled cells may provide a powerful multimodal tool that merges structural and functional information of micrometer-sized biological samples.

References/Acknowledgement: [1] Duyn J *et al*, PNAS 2007; 104(28):11796-801. [2] Marques JP *et al*, NMR in Biomed 2009; 46(2):345-52. [3] Lin YJ *et al*, MRM 1997; 38:378-388. [4] Baxan N *et al*, ISMRM 2010, # 731. This work was supported by the European Union (FP6-NEST-2004: Micro-MR).